DOI: 10.18727/0722-6691/5067

APEX Band 9 Reveals Vibrationally Excited Water Sources in Evolved Stars

Alain Baudry[1]
Fabrice Herpin[1]
Elizabeth Humphreys[2]
Karl Torstensson[2]
Wouter Vlemmings[3]
Anita Richards[4]
Malcolm Gray[4]
Carlos De Breuck[2]
Michael Olberg[3]

[1] Laboratoire d'astrophysique de Bordeaux, Université de Bordeaux, France
[2] ESO
[3] Onsala Space Observatory, Department of Space, Earth and Environment, Chalmers University of Technology, Sweden
[4] Jodrell Bank Centre for Astrophysics, University of Manchester, UK

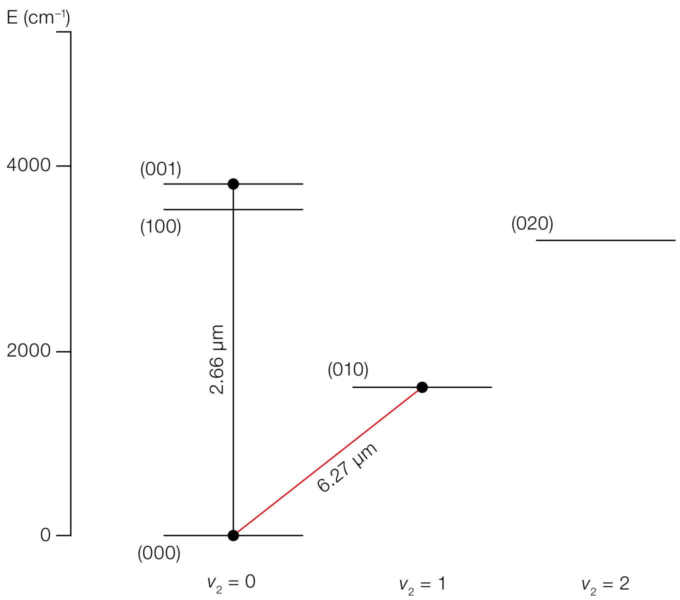

Figure 1. Vibrational energy diagram of water showing all states up to about 4000 cm^{-1}. The states are ordered along the horizontal axis according to the second vibrational state v_2. We show the two main vibrational transitions from the ground-state ($v_1 = 0$, $v_2 = 0$, $v_3 = 0$) to (010) and to (001) around 6.27 and 2.66 µm. The infrared transitions correspond to symmetric bending and anti-symmetric stretching of the water molecule. The 658 GHz rotational transition lies in the (010) state.

We have used the Atacama Pathfinder Experiment (APEX) telescope with the sensitive Swedish-ESO PI APEX (SEPIA) Band 9 receiver to discover several new vibrationally excited line sources of water at 658 GHz in the atmosphere of selected O-rich evolved stars. We have shown that this transition is masing and can be used to probe the gas in the dust formation zone or the wind beyond the central star. The 658 GHz line is widespread in evolved stars but most sources are weaker than about 300–500 Jy. However, some exceptional cases reach up to a few thousand Jy. New models incorporating several vibrationally excited transitions of water allow us to predict the physical conditions prevailing in 658 GHz sources. The strongest ones could be mapped with ALMA to study the small-scale clumpiness of the gas in the dust formation zone or, more generally, the stellar wind.

Water: a masing molecule and ubiquitous tracer of stellar evolution

Evolved objects such as asymptotic giant branch (AGB) and red supergiant (RSG) stars undergo strong mass loss (10^{-6} to 10^{-4} $M_{\odot}$ yr^{-1}) before they reach the white dwarf or supernova stage. Several mechanisms –0 for example shocks which can levitate stellar material, or radiation pressure on dust which drags the gas outwards – compete with gravity during the late stages of stellar evolution to shape circumstellar envelopes. Magnetic fields or nearby companions may also play a role in this shaping process. Owing to the presence of shocks and stellar winds, complex chemistry is observed in the extended atmospheres and the circumstellar envelopes of AGBs or RSGs (for example, Justtanont et al., 2012; Alcolea et al., 2013).

Among all of the molecules that have been identified towards evolved stars, water plays a prominent role because multiple infrared and radio wavelength transitions can be used to probe the physical conditions and kinematics in these stars. A first demonstration of the presence of water in the atmosphere of O-rich evolved stars was provided by the low-dispersion identification of vibrational transition bands in the 1–3 µm domain (for example, Spinrad & Newburn, 1965). To probe the layers of stellar atmospheres more precisely one needs to observe pure rotational transitions of H_2O in the radio domain with heterodyne receivers.

Strong 22 GHz emission from the $J = 6_{16}–5_{23}$ rotational transition of ortho-water in the (000) ground vibrational state was first reported by Cheung et al. (1969) toward Orion. Since then, 22 GHz emission has been observed in hundreds of young star-forming regions and evolved stars (for example, Kim et al., 2014). The 22 GHz line emission is often peculiar: the spectral features can be very narrow, polarised and time variable. In addition, Very Long Baseline Interferometry (VLBI) observations demonstrate that line brightness temperatures may reach about 10^{12} K in some RSGs. Such a high, non-thermal temperature is typical of maser action. Maser emission from various rotational levels above 640 K of the 22 GHz transition was also detected with various radio telescopes toward several evolved stars.

Most of these rotational lines of water can be explained by collisional pumping or by a combination of collisional and radiative pumping models. Recently, Gray et al. (2016) included energy levels up to the (020) vibrational state lying some 4500 K (about 3150 cm^{-1} or 3.17 µm) above the ground vibrational state (Figure 1). Because of the large near-infrared flux density in evolved stars, rotational transitions in the populated (010) and (020) vibrational states should be detectable and can be used to probe the physical conditions and dynamics of specific regions around stellar sources more thoroughly. Several rotational transitions of H_2O in the (010) state have been observed in the radio domain (see Table 1 in Gray et al., 2016). However, these lines tend to be weak, with the exception of the transition discussed here; the $J = 1_{10}–1_{01}$ rotational transition of ortho-water at 658 GHz lies in the (010) state about

Source name	Variabilty	Reference	Source name	Variability	Reference
WX Psc	OH/IR	5	S Vir	Mira	1
R Aql	Mira	4	W Hya	Mira	3, 2, 1, 5
o Ceti	Mira	5,2	RU Hya	Mira	2
R Cet	Mira	1	RX Boo	SR	3
R Hor	Mira	2	S CrB	Mira	3
RT Eri	Mira	2	V351 Nor	LP variable	1
IK Tau	Mira	4, 5, 2	IRAS 15568-4513	IR source	1
U Men	SR	1	U Her	Mira	3
R Dor	SR	5, 1	V446 Oph	SR	1
R Cae	Mira	1	V1006 Sco	SR	1
IRAS 05052-8420	AGB	1	AH Sco	RSG	2
TX Cam	Mira	4, 5	RW Sco	Mira	1
T Lep	Mira	1	V1019 Sco	SR	1
U Dor	Mira	1	V4201 Sgr	SR	1
S Pic	Mira	1	VX Sgr	RSG	3
R Oct	Mira	1	RAFGL 5552	RSG?	1
U Ori	Mira	4	R Aql	Mira	4
L2 Pup	SR	1	V342 Sgr	Mira	1
V578 Pup	Mira	1	GY Aql	SR	1
VY CMa	RSG	3, 2, 4, 8, 9	V2234 Sgr	AGB	1
OH231.8+4.2	PPNebula	6	X Pav	SR	2
KK Car	Mira	1	T Mic	SR	1
RW Vel	Mira	1	NML Cyg	RSG	3, 7
RS Vel	Mira	1	IRAS 20541-6549	AGB	1
IW Hya	Mira	1	R Peg	Mira	1
R Leo	Mira	3, 4	R Aqr	Mira	1
IRAS 10323-4611	C star	1	R Cas	Mira	4, 5
R Crt	SR	3			
RT Vir	SR	3, 2	OH26.5+06	AGB	5
R Hya	Mira	4, 2	RAFGL 5379	AGB	5

Table 1. A complete list of stars detected in the vibrationally excited line of ortho-water at 658 GHz (as of September 2017). Stellar sources are ordered by right ascension with two weak detections added at the end. Mira, RSG and SR stand for Mira-type, red supergiant and semi-regular variability respectively. OH/IR variability means the O-rich AGB star has an unknown or uncertain period of variability. References are: 1 This work; 2 Baudry et al. (2018); 3 Menten and Young (1995); 4 Hunter et al. (2007); 5 Justtanont et al. (2012); 6 Bujarrabal et al. (2012); 7 Teyssier et al. (2012); 8 Alcolea et al. (2013); 9 Richards et al. (2014).

1640 cm^{-1} or 2360 K above the ground-level, and was first detected in variable stars and two RSGs (Menten & Young, 1995).

Widespread 658 GHz line emission toward evolved stars

Several years after the discovery by Menten and Young (1995), observations using the Submillimeter Array (SMA) and Herschel Space Observatory with the Heterodyne Instrument for the Far-Infrared (HIFI) expanded the number of sources detected at 658 GHz to 19 evolved, variable stars (Hunter et al., 2007; Justtanont et al., 2012). Weak emission was also detected with HIFI from two AGB stars (Justtanont et al., 2012) and from one protoplanetary nebula (Bujarrabal et al., 2012). These observations suggested that 658 GHz stellar sources are widespread. Along with our models, which predict that the 658 GHz line can be strongly masing, this suggests that the Atacama Large Millimeter/submillimeter Array (ALMA) could map the most interesting sources.

With this in mind, we built a small catalogue consisting of nearly 100 candidate and known 658 GHz southern sources. The sample is based on stars with known H_2O (22 GHz) and SiO (43 and/or 86 GHz) maser emission above a fixed flux density limit of ~ 50 Jy. SiO emission is important because it is present in many O-rich evolved stars, and SiO and 658 GHz H_2O excitation levels are close to each other (~ 1800 and 2360 K, respectively). A large fraction of our selected sources comes from a homogeneous sample that was simultaneously observed in SiO and H_2O (22 GHz) by Kim et al. (2010). Additional sources were added from the published literature using the same selection criteria in order to improve the coverage in declination.

We used the APEX telescope, using the dual-sideband and dual-polarisation Band 9 Swedish-ESO PI receiver for APEX (SEPIA; Belitsky et al., 2017). The receiver was tuned to place the 658 GHz water line and the J = 6–5 line of ^{13}CO at 661 GHz in the lower sideband where the atmospheric transparency is better. APEX is the only telescope other than ALMA that is currently equipped to observe at 658 GHz.

In our first observing campaign (from April to June 2016) we used SEPIA Science Verification time to observe nine AGB stars and one supergiant source. All ten sources were detected, half of which were new discoveries (Baudry et al., 2018). In a second observing campaign (from July to September 2017), 39 other sources from our sample of late-type stars were observed with the fully commissioned SEPIA receiver. Both runs had good observing conditions with precipitable water vapour below 0.7 mm. A total of 31 new 658 GHz sources were detected (most of them are shown in Figure 2). Our 2016 and 2017 results more than double the number of stars known to exhibit 658 GHz emission, demonstrating that this water transition is widely excited in evolved O-rich stars. All our data were reduced using the Continuum

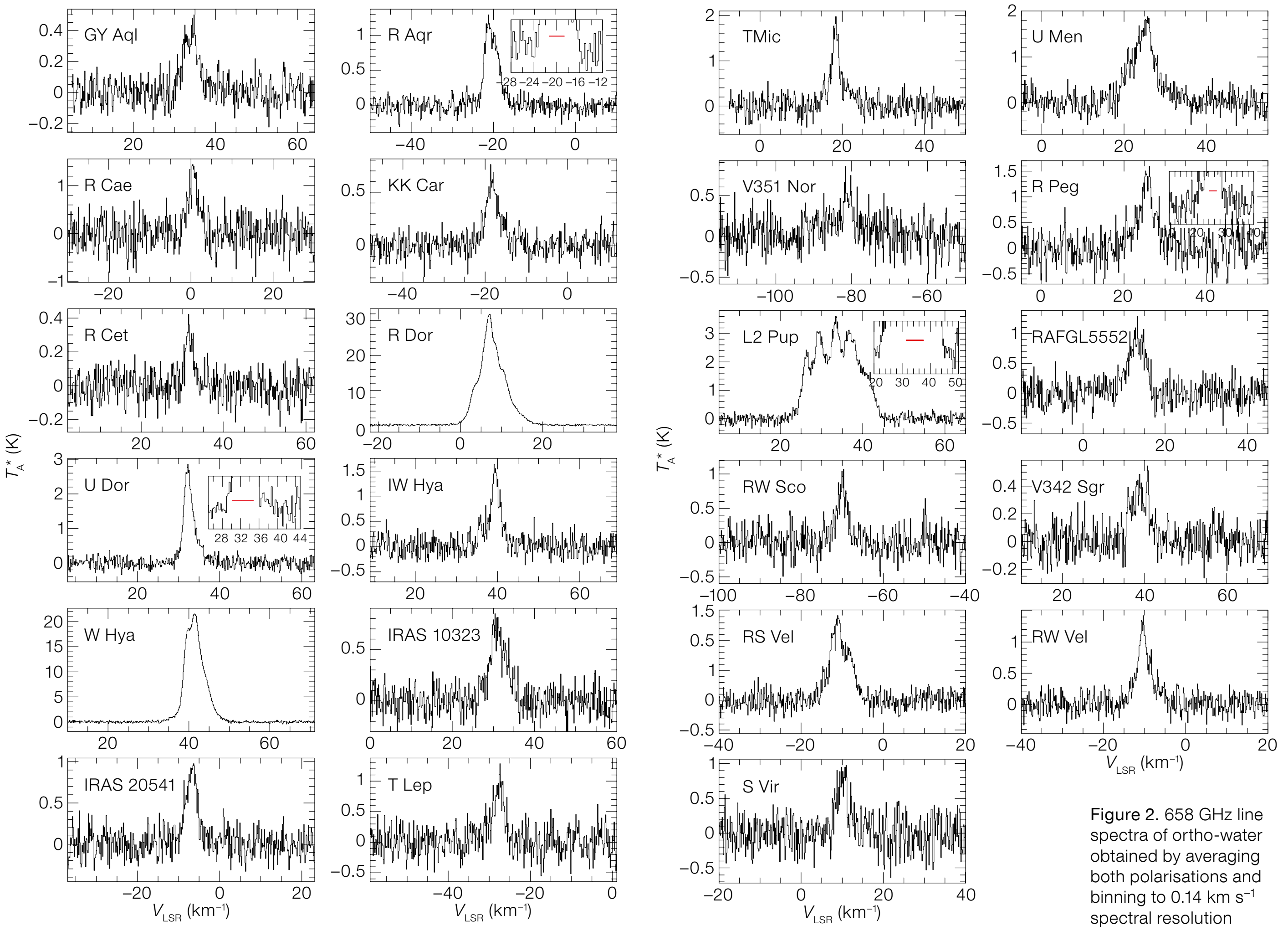

Figure 2. 658 GHz line spectra of ortho-water obtained by averaging both polarisations and binning to 0.14 km s^{-1} spectral resolution towards O-rich stars observed with APEX in 2017; one of the stars IRAS10323-4611 is C-rich.

and Line Analysis Single-dish Software (CLASS) software package[1].

The 658 GHz line profiles are smooth and centred close to the stellar velocity. However, the strongest sources can exhibit asymmetrical line profiles and are likely due to maser emission as explained below. The line widths at half intensity are a few km s^{-1}, with the exception of the supergiant VY CMa (~ 11 km s^{-1}) and the peculiar AGB L2 Pup (~ 14 km s^{-1}). The observed peak line intensities in Figure 2 are given in terms of the antenna temperature, T_A^*, and corrected for absorption due to the Earth's atmosphere, which allows them to be converted into source flux densities. Observations show variations in T_A^* from 0.3–0.4 K for the weakest sources, up to about 31.8 K for R Dor. We derive a flux density to

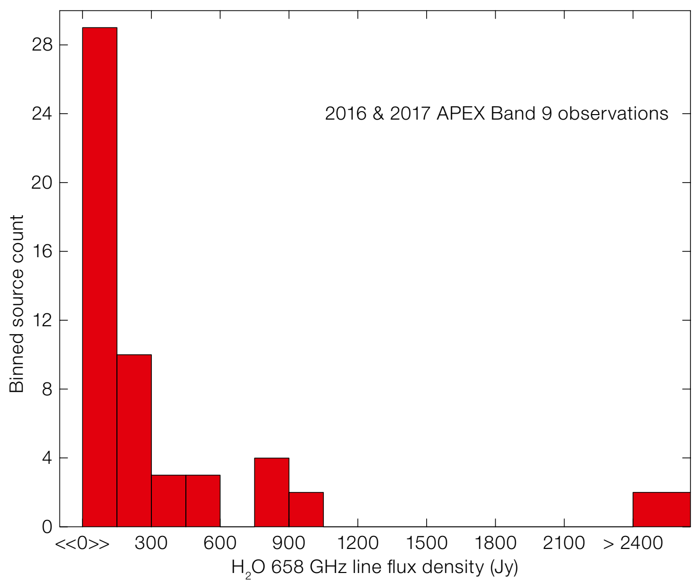

Figure 3. Histogram showing the 658 GHz line flux density of ortho-water for all sources observed with APEX in 2016 and 2017. The first bin from <<0>>–150 Jy starts at the 3-σ level, at ~ 29 Jy.

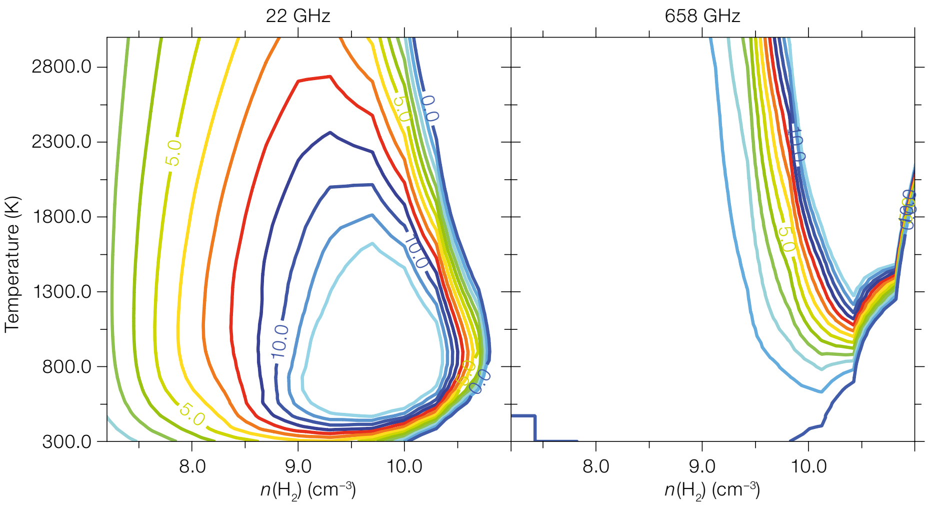

Figure 4. Maser negative optical depth contours for the 22 and 658 GHz lines in the kinetic temperature versus H_2 density plane according to Gray et al. (2016) modelling. Contours are equally spaced up to the maximum value of 12.

antenna temperature conversion factor of 120 (± 10) Jy K^{-1} from 2017 (unresolved) Uranus observations. The observed source flux density varies from ~ 40–3800 Jy, a broad range which partially reflects different distances to the sources, and is partially due to different maser line amplification processes or stellar activity. Nearly all sources are weaker than 300–500 Jy. Figure 3 shows the histogram of 658 GHz flux density for all of our sources, which has a peak below 150 Jy. Table 1 lists the variability characteristics of all evolved stars for which there are 658 GHz water line detections (as of September 2017).

On the masing nature of the 658 GHz emission

We do not think that the 658 GHz line is thermally broadened and excited for several reasons. First, the line width at half-intensity (which is broader than the expected 2–2.5 km s^{-1} thermal line width) remains small compared to the typical 10 to 20 km/s line width of the ^{13}CO, J = 6–5 line requiring hot gas conditions (compared to low-J CO emission). And, for most stars, the 658 GHz line width at half-intensity remains small compared to the low-J CO line width. Secondly, since the flux density of the 658 GHz transition can reach several thousand Jy we may infer that the line brightness temperature T_b(658) is well above the gas kinetic temperature (though our single dish observations only provide weak constraints).

In the unique case of VY CMa Richards et al. (2014) were able to map the 658 GHz emission with ALMA and identify gas "clumps" with brightness temperatures above 0.3–4 × 10^7 K. The nearly contemporaneous 22 and 658 GHz observations of Menten and Young (1995) can be used to constrain T_b(658) in other evolved stars. Assuming that both emissions at a given spectral velocity are excited in comparable gas volumes, we expect values of T_b(658) ~ 10^4–10^{10} K from 22 GHz observations of AGBs. This clearly indicates suprathermal emission and maser action for VY CMa and AGBs.

Finally, the multi-level, radiative transfer calculations applied to physical conditions and material slabs typical for evolved stars show that the 658 GHz line can be inverted and masing (Gray et al., 2016). In Figure 4 we compare the physical conditions leading to 22 and 658 GHz maser emission. Negative 658 GHz opacities as high as 10 are reached for kinetic temperatures from 1000–2800 K or over and for densites of ~ 10^{10} cm^{-3}, suggesting layers of material that are relatively close to the stellar photosphere.

Figure 4 also shows that the loci of inverted 22 GHz line emission are broader than those at 658 GHz. This is expected for a transition which is both collisionally and radiatively excited and thus easily detected in a variety of physical environments. Along with the high-energy levels at 658 GHz, it appears likely that the 658 GHz line is formed in layers close to the photosphere. The 658 GHz map of VY CMa (Richards et al., 2004) showed that the broad aggregate line profile is made up of several spatially and spectrally distinct gas clumps. The narrower spectral features are distributed within 50–250 milliarcseconds of the central star in a region where SiO masers are also present.

It is possible to prove indirectly that the 658 GHz emission is excited close to the star by comparing the 658 GHz velocity extent at "zero" intensity with the same quantity for the SiO maser emission at 86 GHz in the first vibrational state for a small sub-sample (Baudry et al., 2018). This can be justified because: a) the SiO v = 1 state energy is around 1800 K and close to the (010) vibrational state of the 658 GHz line; b) the emission peak velocities of both maser lines are close to each other; and c) VLBI observations indicate that SiO masers are formed within ~ 5 R* of the central object. The loose correlation found (see Figure 5) suggests that both masers are excited in similar environments close to the central star, but this should be confirmed with a larger sample.

In a few stars, the 658 GHz line width to 'zero' intensity (defined as the width down to 2- to 3-σ spectral noise) is comparable to that measured for CO, which traces the circumstellar envelope expansion. In four stars — R Aqr, U Dor, L2 Pup and R Peg — the 658 GHz low-level emission is broader than the corresponding CO velocity extent; see horizontal, red bar in Figure 2 for CO, J = 2–1 velocity extent from Groenewegen et al. (1999), Kerschbaum & Olofsson (1999) and Winters et al. (2002). This low-intensity emission is unlikely to trace the envelope expansion in regions that are cooler than required to excite the 658 GHz line. On the other hand, it could be related to gas acceleration close to the central star and/or perhaps to shocks; this is also supported by 658 GHz filaments observed by ALMA in VY CMa. Even if the bulk of the 658 GHz emission is masing we cannot exclude the possibility that the low-intensity radiation is due to weak thermal excitation of the gas.

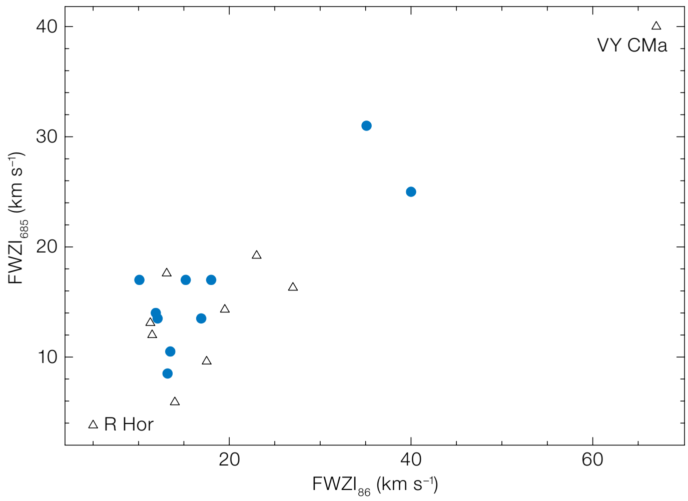

Figure 5. Full width at zero intensity (FWZI) at 658 GHz (vibrationally excited H_2O) *versus* FWZI at 86 GHz (SiO, v = 1 maser) for 10 sources (triangles) observed in Baudry et al. (2018) and 10 additional sources. The R Hor and VY CMa labels mark the two ends of the observed loose correlation.

Time variability, light amplification and future plans

Molecular line masers, especially the 22 GHz H_2O line, often exhibit time variability and narrow spectral features, resulting from the population inversion and radiation amplification mechanisms. These properties are not immediately obvious with our single-dish observations of the 658 GHz line. In two well-studied cases, VY CMa and W Hya, which have been observed over more than 20 years, the emission line profiles have remained stable and asymmetric, though there is a regular decline of the peak intensity in the VY CMa observations. In Baudry et al., (2018) we also showed that, by comparing the ratio of the H_2O(658) to ^{13}CO(6–5) integrated intensities nearly six years apart, we could not reconcile the measurements in three stars (o Ceti, IK Tau and W Hya). This suggests time variability at 658 GHz and, indirectly, maser action — since the high-*J* ^{13}CO broad line profile related to circumstellar expansion should not change rapidly.

The 658 GHz line width of individual masers depends on the light amplification regime within the material in which the H_2O population is inverted. If the radiation grows with the exponential of the 658 GHz opacity as expected for unsaturated masers, we may observe rapid time variability and line features that are smaller than the local thermal line width. At the other extreme, maser saturation corresponds to an intrinsic maximum luminosity resulting in little or no time variability and the individual maser line features may be as broad as the local thermal width. The 658 GHz single-dish observations do not show spectral features as narrow as the expected thermal line widths because the multiple 658 GHz velocity–blended components forming the overall line profile within the 9-arcsecond beam of APEX remain unresolved. These components can only be separated by mapping their emission (for example, VY CMa; Richards et al., 2014).

Our APEX results suggest that strong 658 GHz line sources could be mapped with ALMA to reveal the details of the kinematics and the small-scale clumpiness of stellar winds within the dust formation zone and beyond. In the case of the supergiant VY CMa, ALMA showed that the 658 GHz emission extends further out of the dust formation zone. However, we do not know if this property, which likely traces shocks in the stellar envelope, is specifically due to its exceptionally strong winds (VY CMa's mass loss rate ~ 2×10^{-4} M yr^{-1}). 658 GHz images obtained at different epochs for some sources could also tell us how gas clumps evolve with time, which ones show variable activity, and more generally, how stellar winds evolve. Finally, we note that this transition may be suitable for ALMA Band 9 phase calibration, given the relatively simple line shapes and strength of the 658 GHz emission in stars for which coordinates are well known. Compact (< 0.35 arcseconds) and strong 658 GHz emission was detected towards the massive protostar Orion Source I in the Orion KL region (Hirota et al., 2016), and could also be used for phase calibration.

Acknowledgements

Our data were acquired with the APEX telescope equipped with the Swedish-ESO Band 9 receiver. APEX is a collaboration between the Max-Planck-Institut für Radioastronomie, ESO and the Onsala Space Observatory. We warmly thank the APEX staff who carried out the APEX SEPIA Band 9 observations.

References

Alcolea, J. et al. 2013, A&A, 559, 93
Baudry, A. et al. 2018, A&A, 609, 25
Belitsky, V. et al. 2017, arXiv171207396B
Bujarrabal, V. et al. 2012, A&A, 537, 8
Cheung, A. C. et al. 1969, Nature, 221, 626
Gray, M. D. et al. 2016, MNRAS, 456, 374
Groenewegen, M. A. T. et al. 1999, A&AS, 140, 197
Hirota, T. et al. 2016, ApJ, 817, 168
Hunter, T. R. et al. 2007, IAU Symposium, 242, 471
Justtanont, K. et al. 2012, A&A, 537, 144
Kerschbaum, F. & Olofsson, H. 1999, A&AS, 138, 299
Kim, J. et al. 2010, ApJS, 188, 209
Kim, J. et al. 2014, AJ, 147, 22
Menten, K. M. & Young, K. 1995, ApJ, 450, L67
Richards, A. M. S. et al. 2014, A&A, 572, L9
Spinrad, H. & Newburn, Jr. R. L. 1965, ApJ, 141, 965
Teyssier, D. et al. 2012, A&A, 545, 99
Winters, J. M. et al. 2002, A&A, 308, 609

Links

[1] CLASS software package: http://www.iram.fr/IRAMFR/GILDAS